

Preparation of silver/chemically reduced graphene composite for flexible printed circuits

Bin Feng^{1,2} ✉, Junjie Ma¹, Xiaolong Gu¹, Xinbing Zhao², Yu Zhang¹

¹Zhejiang Province Key Laboratory of Soldering & Brazing Materials and Technology, Zhejiang Metallurgical Research Institute Co., Ltd., Hangzhou 310030, People's Republic of China

²State Key Laboratory of Silicon Materials and Department of Materials Science and Engineering, Zhejiang University, Hangzhou 310027, People's Republic of China

✉ E-mail: Binfeng@asia-general.com

Published in *Micro & Nano Letters*; Received on 29th August 2017; Revised on 27th December 2017; Accepted on 8th January 2018

Silver (Ag)/chemically reduced graphene (Ag/CGN) composite succeeded prepared using a simple chemical reduction method. X-ray diffraction, Raman spectra, Fourier transform infrared spectroscopy and X-ray photoelectron spectroscopy results revealed the formation of Ag and the reduction of graphite oxide to graphene during the synthesis process. Scanning electron microscopy observation showed that Ag particles were wrapped by graphene. The resistance of Ag/CGN circuits changed <10% when bended at a radius of 10 mm after 500 cycles and <15% when folded after 50 cycles, indicating the printed Ag/CGN fine circuits possess good electrical conductivity, flexibility and electrical stability under mechanical deformations. Furthermore, the Ag/CGN circuits exhibited high thermal stability, indicating its potential application for fabricating high performance flexible printed circuits.

1. Introduction: In the last decade, there has been an explosive growth of flexible printed circuits and devices, such as flexible touch panels [1], radio frequency identification [2], sensors [3], wearable electronic devices [4], solar cells [5] and organic light emitting device [6]. Developing conductive pastes is particularly important for flexible printed circuits because screen printing is an effective approach for mass production with low environmental impact and low cost [7]. Traditionally, silver (Ag) is the preferred conductive phase for most conductive pastes because of its considering merits such as high electrical conductivity and stability. However, owing to the rareness and high price of Ag, there is an urge demand to develop appropriate alternatives for Ag. Moreover, the new conductive phase should possess comparable performances with Ag when used in conductive pastes.

Copper (Cu) has long been regarded as the most promising alternative material because it has a comparable conductivity to silver while it's much cheaper [8]. However, Cu shows poor oxidation resistance, which prevents the copper conductive paste from wider applications. Carbon materials are also considered to replace Ag by many researchers. Although carbon based conductive pastes [9, 10] exhibit good stability, their electrical conductivity is not good enough. Especially, graphene has shown its potential in printed circuits [11]. Apart from these two choices, composite consist of Ag and carbon materials is another effective substitute, which has been shown viable by other researchers [12–15].

Compared with other carbon materials, graphene, a two-dimensional (2D) sp²-bonded carbon material, is an ideal matrix of composite owing to its appealing characteristics, such as high electronic conductivity [16], high specific surface area [17] and good flexibility [18]. Herein, we report a simple preparation of Ag/chemically reduced graphene (Ag/CGN) and demonstrate its use for the flexible printed circuit. The Ag/CGN composite was made into a conductive paste. After screen printing and curing, the composite formed electrodes as a part of circuits. The results showed that conductive paste contains this composite possess low resistance as well as enormous flexibility after cured, indicating that the Ag/CGN composite is competent for flexible printed circuit.

2. Experiments: In a typical procedure, graphite oxide (GO, 50 mg), purchased from Nanjing XFNANO Materials Tech Co. Ltd., was ultrasonically dispersed in 50 ml of deionised water for 2 h to form a uniform dispersion. Then, 1.25 mmol of AgNO₃ and 1.25 mmol citric acid were added to the above solution. After being stirred for 2 h, the desired amount of N₂H₄·H₂O was slowly added followed by a rapid agitate for another 0.5 h. The resulting product was collected by centrifugation, washed with deionised water for several times and dried at 40°C in a vacuum oven. A control experiment was also carried out to prepare bare Ag using the same route without adding GO. Bare graphene was also synthesised using GO as the precursor.

The crystal structure of the obtained products was identified by X-ray diffraction (XRD) on a Bruker D8 Advance powder diffractometer. Raman spectra were recorded on a Jobin-Yvon Labor Raman HR-800. Fourier transform infrared (FTIR) spectroscopy tests were conducted on a Nicolet 6700 Fourier infrared spectrometer. X-ray photoelectron spectroscopy (XPS) measurements were performed on a KRATOS AXIS ULTRA-DLD spectrometer with a monochromatic Al K α radiation ($h\nu=1486.6$ eV). The carbon content analysis was conducted on a CS-2800 carbon sulphur analyser. The microstructure of the samples and the thickness of the traces were characterised by field emission scanning electron microscopy (SEM) on an EIGMA microscope. Sheet resistance was measured by an RTS-8 four-probe meter at 25°C.

3. Results and discussions: Fig. 1a gives the XRD patterns of the resultant products: Ag/CGN composite and pure Ag. For both samples, all the diffraction peaks of Ag/CGN and bare Ag match well with the standard patterns of Ag (space group Fm3m, JCPDS Card No. 04-0783). No diffraction peak of GO can be observed in Ag/CGN composite indicating that GO was converted into graphene during the synthesis procedure [19]. The diffraction peaks corresponding to graphene is also undetected, which indicated that the reassembly of the graphene sheets after reduction is restricted by firmly deposited Ag particles in between the graphene sheets. The content of graphene in Ag/CGN composite was estimated to be 1 wt% by carbon content analysis.

To check whether the GO was reduced to graphene, Raman spectra were conducted. Fig. 1b shows the Raman spectra of

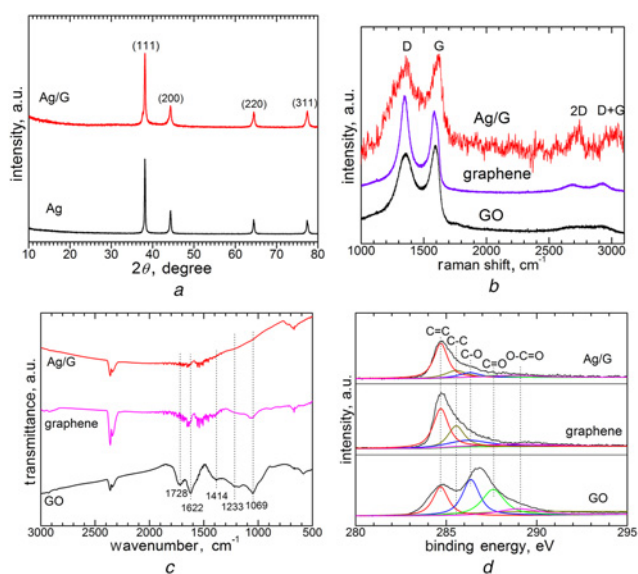


Fig. 1 Materials characterisations of different samples
 a XRD patterns of Ag/CGN and bare Ag
 b Raman spectra of Ag/CGN, graphene and GO
 c FTIR spectra of Ag/CGN, graphene and GO
 d C1s XPS of Ag/CGN, graphene and GO

Ag/CGN, bare graphene and GO. All the three samples present two characteristic bands, the G peak at around 1590 cm^{-1} and the D peak at around 1350 cm^{-1} [20]. For GO, the D-to-G peak intensity ratio (I_D/I_G) is estimated to be 0.79. Compared to GO, both Ag/CGN and graphene exhibit an increased D/G intensity ratio. I_D/I_G for graphene in Ag/CGN and bare graphene are 1.08 and 1.11, respectively. The increased D/G intensity ratio was caused by a decreased average size of the sp^2 domains and an increased number of these domains, indicating the reduction of GO to graphene [17]. In addition, two peaks corresponding to 2D [21] peak and D+G peak [22] of carbon materials at around 2700 and 2900 cm^{-1} were also observed. The Ag/CGN composite shows a wide 2D peak, which means graphene is in few layer form [20]. This phenomenon was also reported by other researchers [23, 24]. And according to Geim [25], one of the discoverers of graphene, 'graphene' can be divided into three types: single, double, and few layers (3–10 layers). Therefore, the graphene in Ag/CGN can be treated as 'graphene' in few layer form.

The reduction of GO was also proved by FTIR as shown in Fig. 1c. Two feature absorption bands of GO were observed, the obvious absorption band at 1728 cm^{-1} related to the C=O stretching and the band around 1622 cm^{-1} owing to aromatic C=C [26]. While the bands at 1412 , 1233 and 1069 cm^{-1} correspond to carboxy C–O, epoxy C–O and alkoxy C–O, respectively [26]. Note that there is a distinct decreasing of peak intensity associated to C=O and C–O for Ag/CGN and graphene, indicative of a remarkable reduction of GO after the solvothermal reactions, agreeing well with the Raman results.

Fig. 1d compares the C1s XPS of Ag/CGN, graphene and GO. The results are fitted into five peaks. For the graphite oxide, the carbon in C–O bonds (286.3 eV), carbonyl carbon (C=O, 287.6 eV) and carboxylate carbon (O–C=O, 289.0 eV) all exhibit a high intensity, indicating considerable oxidation of graphite [27]. After the reduction reaction, the peak intensity of carbons in C–O, C=O and O–C=O shows a remarkable decrease, confirming that a sufficient reduction of GO to graphene has occurred [17, 27]. It should be stressed that residual epoxide and/or hydroxyl groups exist because groups situated at the edges of the GO are difficult to remove which is in agree with the theoretical calculation [28].

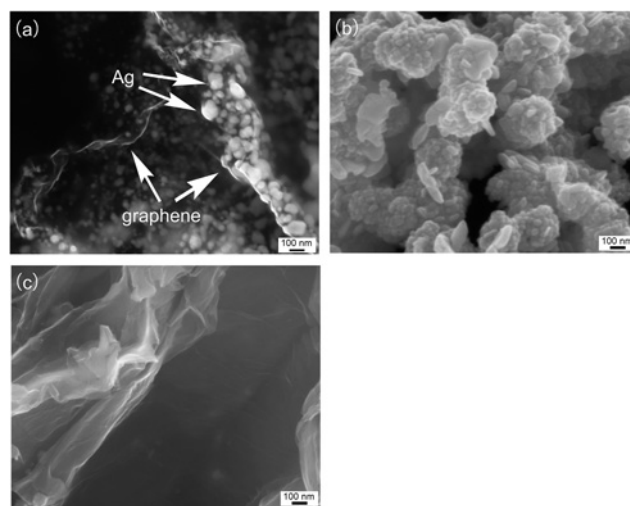


Fig. 2 SEM images of two samples
 a Morphology of Ag/CGN composite
 b Morphology of bare Ag
 c Morphology of bare graphene

Fig. 2 gives the SEM images of Ag/CGN composite and pure Ag. The typical morphology of Ag/CGN composite is shown in Fig. 2a. The graphene sheet, as denoted by the arrows, exhibits a transparent feature indicating that it is rather thin. Through the transparent graphene, it can be seen clearly that Ag particles are wrapped by the graphene sheets. Without the confinement of graphene, bare Ag particles tend to aggregate as shown in Fig. 2b. Fig. 2c exhibits the morphology of bare graphene. The graphene sheets also show a transparent feature. However, graphene seems to be thicker than that in Ag/CGN sample. This may due to restacking of graphene sheets.

The conductive paste consists of Ag/CGN composite, resin and an organic solvent. Typically, organic solvent and resin were stirred in a three-necked round-bottom flask at 90°C . After mixed for 10 h, cooled the mixture to the room temperature. Subsequently, the Ag/CGN composite was introduced into the mixture by mixing for 3 min to obtain a homogeneous conductive paste. The paste was then passed through a triple roller mill to break the agglomerates. Repeat the above procedure until the fineness of the paste is under $10\text{ }\mu\text{m}$. After screen printing, the paste was transferred to a PET substrate. And the curing procedure was completed at 150°C for 0.5 h.

The average sheet resistance of the printed films after cured was $33\text{ m}\Omega/\text{sq}/25\text{ }\mu\text{m}$. Fig. 3a shows that a fine line with a width of $300\text{ }\mu\text{m}$ could be fabricated, and no cracks were observed in the cured trace. The traces were linked with an LED. When electrified the trace, the LED was lighted, demonstrating the conductivity of the traces, as shown in Fig. 3a. To prove the flexibility of the printed conductive track, it was bent and used as a conductive wire to light up an LED, as shown in Fig. 3b. The lighted LED visually demonstrated that when a large deflection bending was applied to the Ag/CGN conductor, the LED still light under the deformation of bending. Furthermore, even when we 180° folded the Ag/CGN conductive circuits as displayed in Fig. 3c, the LED was still lighted, indicating that the printed Ag/CGN fine circuits possess good electrical conductivity, flexibility, and electrical stability under mechanical deformations.

Fig. 4a compares the normalised resistance of printed conductive track on PET as a function of the number of bending cycles at a bend radius of 10 and 20 mm and each cycle comprised one stretching and compressing of the Ag/CGN circuits. When the bend radius was 20 mm, the resistance of the trace only increased 1% after 500 cycles. When the bend radius was reduced to 10 mm, the resistance

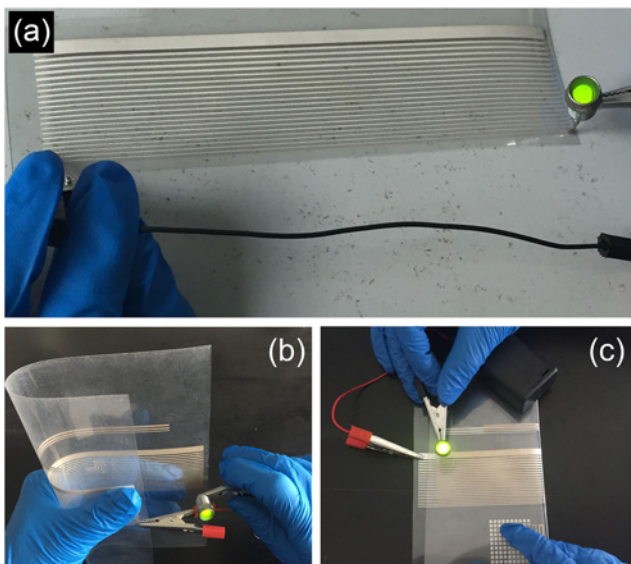


Fig. 3 Photos of the printed Ag/CGN electrical circuits with attached LEDs on various situation
 a Printed fine line with a width of 300 μm
 b Bended PET film
 c Folded PET film

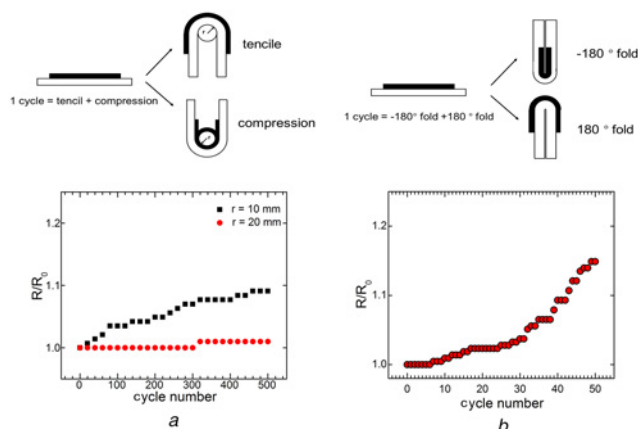


Fig. 4 Scheme showing the test mode of the Ag/CGN circuits (top) and normalised resistance of the Ag/CGN circuits at different test mode (bottom)
 a Bending test
 b Folding test

increased <10% after 500 bending cycles. In the folding tests, the foldability of the Ag/CGN circuits was evaluated by measuring the resistance while folding the samples at an angle of -180° and 180° , as depicted in Fig. 4b. The resistance increased slowly in the first 30 cycles, of which R/R_0 was 1.04 after 30 cycles. More drastic resistance increases were found after more bending cycle tests. After 50 cycles, the resistance increased 15%. Low resistance variation for bending and folding test indicating that the printed Ag/CGN fine circuits possess good flexibility.

The thermal stability of Ag/CGN trace was also checked. The PET film with Ag/CGN traces was put in an oven at 80°C to evaluate the reliability of the Ag/CGN circuits. As demonstrated in Fig. 5a, the resistance of Ag/CGN circuits remain unchanged for the first 5 days and gradually decreased to $20\text{ m}\Omega/\text{sq}/25\ \mu\text{m}$ after 180 days. It is surprising that the resistance of Ag/CGN circuits did not increase with the increasing time, but decreased a lot, indicating that the electrical property improved during aging test. This might be attributed to resin shrinking at high temperature, which

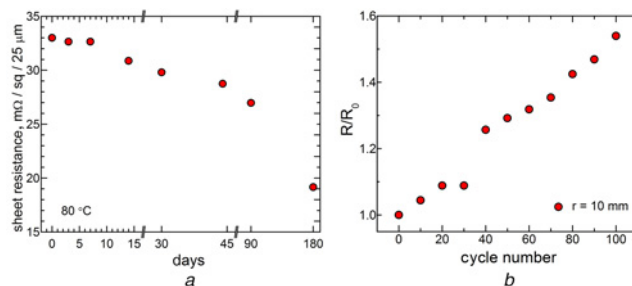


Fig. 5 Thermal stability test results of Ag/CGN circuits
 a Sheet resistance of the Ag/CGN circuits versus days at 80°C
 b Normalised resistance of the Ag/CGN circuits versus bending cycles after aging

provides a stronger mechanical interconnection to the Ag/CGN composites. The sample was also conducted bending tests to evaluate its flexibility after high temperature. As shown in Fig. 5b, the resistance increased with increasing cycle numbers when bend radius was 10 mm. The resistance increased 54% after 100 cycles. High temperature resulted in fatigue of the Ag/CGN circuits, which caused performance degradation.

4. Conclusion: Ag/CGN composite has been prepared by a facile chemical reduction method. Ag particles were wrapped by graphene. The Ag/CGN composite was used in a flexible printed circuit. The resistance of Ag/CGN circuits changed <10% when bended at a radius of 10 mm after 500 cycles and <15% when folded after 50 cycles, indicating the printed Ag/CGN fine circuits possess good electrical conductivity, flexibility and electrical stability under mechanical deformations. Furthermore, the Ag/CGN circuits exhibited high thermal stability, indicating its potential application for fabricating high performance flexible printed circuits

5. Acknowledgments: This work was supported by the Science and Technology Project of Zhejiang Province (grant no. 2016F50055) and Key Research and Development project of Zhejiang Province (grant no. 2017C01076).

6 References

- [1] Kwon J.: 'Low-temperature oxidation-free selective laser sintering of Cu nanoparticle paste on a polymer substrate for the flexible touch panel applications', *ACS Appl. Mater. Interfaces*, 2016, **8**, (18), pp. 11575–11582
- [2] Putaala J.: 'Capability assessment of inkjet printing for reliable rfid applications', *IEEE Trans. Device Mater. Reliab.*, 2017, **17**, (2), pp. 281–290
- [3] Huang G.W.: 'A paper-based touch sensor with an embedded microprobe array fabricated by double-sided laser printing', *Nanoscale*, 2017, **9**, (27), pp. 9598–9605
- [4] Jeerapan I.: 'Stretchable biofuel cells as wearable textile-based self-powered sensors', *J. Mater. Chem. A*, 2016, **4**, (47), pp. 18342–18353
- [5] Ko S.H.: 'Review of the multi-scale nano-structure approach to the development of high efficiency solar cells', *Smart Sci.*, 2014, **2**, (2), pp. 54–62
- [6] Kim S.J.: 'Study on the fabrication of transparent electrodes by using a thermal-roll imprinted Ag mesh and anatO thin film', *J. Korean Phys. Soc.*, 2016, **68**, (6), pp. 779–785
- [7] Jost K.: 'Knitted and screen printed carbon-fiber supercapacitors for applications in wearable electronics', *Energy Environ. Sci.*, 2013, **6**, (9), pp. 2698–2705
- [8] Tam S.K.: 'High-concentration copper nanoparticles synthesis process for screen-printing conductive paste on flexible substrate', *J. Nanoparticle Res.*, 2015, **17**, (12), p. 12
- [9] Hu K.: 'Dispersion and resistivity optimization of conductive carbon black in environment-friendly conductive coating based on acrylic resin', *Polym. Compos.*, 2015, **36**, (3), pp. 467–474

- [10] Souza V.H.R.: 'Flexible, transparent and thin films of carbon nano-materials as electrodes for electrochemical applications', *Electrochim. Acta*, 2016, **197**, pp. 200–209
- [11] Arapov K.: 'Conductive screen printing inks by gelation of graphene dispersions', *Adv. Funct. Mater.*, 2016, **26**, (4), pp. 586–593
- [12] Wu W.: 'Fabrication, characterization and screen printing of conductive ink based on carbon@Ag core-shell nanoparticles', *J. Colloid Interface Sci.*, 2014, **427**, pp. 15–19
- [13] Hu Y.G.: 'Low cost and highly conductive elastic composites for flexible and printable electronics', *J. Mater. Chem. C*, 2016, **4**, (24), pp. 5839–5848
- [14] Hu P.A.: 'Synthesis of 10 Nm Ag nanoparticle polymer composite pastes for low temperature production of high conductivity films', *Appl. Surf. Sci.*, 2010, **257**, (3), pp. 680–685
- [15] Brusich V.: 'Corrosion and protection of a conductive silver paste', *J. Electrochem. Soc.*, 1995, **142**, (8), pp. 2591–2594
- [16] Novoselov K.S.: 'A roadmap for graphene', *Nature*, 2012, **490**, (7419), pp. 192–200
- [17] Stankovich S.: 'Synthesis of graphene-based nanosheets via chemical reduction of exfoliated graphite oxide', *Carbon*, 2007, **45**, (7), pp. 1558–1565
- [18] Wu Q.: 'Supercapacitors based on flexible graphene/polyaniline nanofiber composite films', *ACS Nano*, 2010, **4**, (4), pp. 1963–1970
- [19] Zhang L.F.: 'Multifunctional Co_{0.85}Se/graphene hybrid nanosheets: controlled synthesis and enhanced performances for the oxygen reduction reaction and decomposition of hydrazine hydrate', *Nanoscale*, 2014, **6**, (3), pp. 1782–1789
- [20] Ferrari A.C.: 'Raman spectroscopy of graphene and graphite: disorder, electron–phonon coupling, doping and nonadiabatic effects', *Solid State Commun.*, 2007, **143**, (1), pp. 47–57
- [21] Ferrari A.C.: 'Raman spectrum of graphene and graphene layers', *Phys. Rev. Lett.*, 2006, **97**, (18), p. 187401
- [22] Rao C.N.: 'Graphene: the new two-dimensional nanomaterial', *Angew. Chem. Int. Ed. Engl.*, 2009, **48**, (42), pp. 7752–7777
- [23] Hsu C.P.: 'Effect of polymer binders in screen printing technique of silver pastes', *J. Polym. Res.*, 2013, **20**, (10), pp. 1–8
- [24] Kim K.S.: 'Large-scale pattern growth of graphene films for stretchable transparent electrodes', *Nature*, 2009, **457**, (7230), pp. 706–710
- [25] Gan W.: 'Investigation of effect of the organic vehicle on performance of front silver paste for solar cell', *New Chem. Mater.*, 2014, **42**, (8), pp. 141–144
- [26] Park S.: 'Colloidal suspensions of highly reduced graphene oxide in a wide variety of organic solvents', *Nano Lett.*, 2009, **9**, (4), pp. 1593–1597
- [27] Shin H.J.: 'Efficient reduction of graphite oxide by sodium borohydride and its effect on electrical conductance', *Adv. Funct. Mater.*, 2010, **19**, (12), pp. 1987–1992
- [28] Gao X.: 'Hydrazine and thermal reduction of graphene oxide: reaction mechanisms, product structures, and reaction design', *J. Phys. Chem. C*, 2010, **114**, (2), pp. 832–842